

Mapping correlated membrane pulsations and fluctuations in human cells

Andrew E. Pelling^{1*}, Farlan S. Veraitch², Carol Pui-Kei Chu², Brian M. Nicholls¹, Alexandra L. Hemsley², Chris Mason² and Michael A. Horton¹

¹The London Centre for Nanotechnology, Centre for Nanomedicine, University College London, 17-19 Gordon Street, London WC1H 0AH, UK

²Advanced Centre for Biochemical Engineering, University College London, Torrington Place, London WC1E 7JE, UK

The cell membrane and cytoskeleton are dynamic structures that are strongly influenced by the thermo-mechanical background in addition to biologically driven mechanical processes. We used atomic force microscopy (AFM) to measure the local membrane motion of human foreskin fibroblasts (HFFs) which were found to be governed by random and non-random correlated mechanical processes. Interphase cells displayed distinct membrane pulsations in which the membrane was observed to slowly contract upwards followed by a recovery to its initial position. These pulsations occurred one to three times *per* minute with variable amplitudes (20–100 pN) separated by periods of random baseline fluctuations with amplitudes of <20 pN. Cells were exposed to actin and microtubule (MT) destabilizing drugs and induced into early apoptosis. Mechanical pulsations (20–80 pN) were not prevented by actin or MT depolymerization but were prevented in early apoptotic cells which only displayed small amplitude baseline fluctuations (<20 pN). Correlation analysis revealed that the cell membrane motion is largely random; however several non-random processes, with time constants varying between ~2 and 35 s are present. Results were compared to measured cardiomyocyte motion which was well defined and highly correlated. Employing automated positioning of the AFM tip, interphase HFF correlation time constants were also mapped over a 10 μm^2 area above the nucleus providing some insights into the spatial variability of membrane correlations. Here, we are able to show that membrane pulsations and fluctuations can be linked to physiological state and cytoskeletal dynamics through distinct sets of correlation time constants in human cells. Copyright © 2007 John Wiley & Sons, Ltd.

Keywords: atomic force microscopy; fluorescence microscopy; autocorrelation analysis; cell membrane fluctuations; apoptosis; cytoskeleton; spatial autocorrelation plots

Received 17 April 2007; revised 11 June 2007; accepted 19 June 2007

INTRODUCTION

At the molecular and cellular length scales (nanometre (nm) to micrometre (μm)) the influence of thermal fluctuations and forces are significant with respect to size and mass. In a simple estimate, the force acting on a cell can be calculated by using Stokes law and estimating the force on the cell by solving the Langevin equation ignoring inertial motion (Strick *et al.*, 2000; Bechhoefer and Wilson, 2002; Smith *et al.*, 2003). By assuming a spherical shape Strick *et al.* have previously estimated that a cell may experience a force of ~10 fN every second from the thermo-mechanical background which is approximately equal to its own weight

(Strick *et al.*, 2000). These forces arise solely from the random Brownian motion of the fluid molecules surrounding the cell at physiological temperatures. Clearly, thermal fluctuations and forces dominate at cellular length scales. One of the still unresolved problems in biology is the determination of how cells and molecules (which may experience forces up to 100 times their own mass) produce highly correlated motions in such a large thermo-mechanical background. Indeed, this area of study is not only important to the understanding of basic biophysics but also has implications for the development of future nanotechnologies which aim to function at the nm scale and within the human body in a wet, physiological environment.

The atomic force microscope (AFM) (Binnig *et al.*, 1986) is an ideal tool to study the mechanical properties and motions of cell membranes that exist in a fluctuating thermal background. With access to nm length scales and pN sensitivity, the AFM cantilever can be used to measure local motions of cell membranes. Several examples of this application have been published previously (Shroff *et al.*,

*Correspondence to: A. E. Pelling, London Centre for Nanotechnology, University College London, 17-19 Gordon Street, London WC1H 0AH, UK.
E-mail: a.pelling@ucl.ac.uk

Abbreviations: AFM, atomic force microscopy; CM, cardiomyocyte; HFF, human foreskin fibroblast; STS, Staurosporine; CytD, Cytochalasin D; PI, propidium iodide; ACF, autocorrelation function; FT, Fourier transform.

1995; Domke *et al.*, 1999; Rotsch *et al.*, 1999; Szabo *et al.*, 2002; Pelling *et al.*, 2004; Pelling *et al.*, 2005; Prass *et al.*, 2006). Some of the earliest published work involved the measurement of highly correlated mechanical contractions of rat atrial myocytes (Shroff *et al.*, 1995) and chicken cardiomyocytes (CMs) (Domke *et al.*, 1999). It was shown that these cells can generate forces in the nanonewton (nN) range and that the material properties of the cell membrane change in response to contraction dynamics (Shroff *et al.*, 1995). In later work, it was observed that *S. cerevisiae* cells, which were not previously known to display any cell wall motions, display physiologically driven, time-dependent nanomechanical oscillations with amplitudes of ~ 3 nm (Pelling *et al.*, 2004; Pelling *et al.*, 2005). Furthermore, in recent work, the protrusive forces generated at the leading edge of the cell membrane of migrating keratinocytes were also measured with AFM and revealed that these forces are significantly greater (~ 2 nN) than the thermal background and are dependent on actin and adhesion dynamics (Prass *et al.*, 2006).

Aside from well correlated motions involving periodic dynamics, random fluctuations of cell membranes have also been observed. In 3T3 cells, fluctuations in membrane height (and elasticity) were observed to increase in migrating cells (Rotsch *et al.*, 1999). In a later study (Szabo *et al.*, 2002), fluctuations of membrane height at the leading and trailing edges of migrating 3T3 cells were also shown to be distinct. The fluctuations were shown to possess a non-random component at ~ 5 Hz. This component was not apparent in regions of the cell with few or no actin stress fibres and it was concluded that the motion may be a result of actin–myosin activity. Finally, several theoretical and experimental approaches have demonstrated that there is a correlation between membrane fluctuations and the dynamics of the underlying cytoskeleton or activity of membrane bound proteins in many cell types (including numerous erythrocyte studies) (Tishler and Carlson, 1987; Bornens *et al.*, 1989; Tishler and Carlson, 1993; Ehrenguber *et al.*, 1996; Yasuda *et al.*, 1996; Tuvia *et al.*, 1999; Pletjushkina *et al.*, 2001; Brown, 2003; Gov, 2004; Gov and Safran, 2005; Gov and Gopinathan, 2006; Lin *et al.*, 2006; Popescu *et al.*, 2006; Silva *et al.*, 2006).

Clearly, there are many approaches to studying membrane fluctuations and the underlying mechanisms driving membrane motion can be complex and are still poorly understood. Membrane fluctuations have generally been related to drastic mechanical processes such as migration, contraction, division or haemolysis (Shroff *et al.*, 1995; Domke *et al.*, 1999; Popescu *et al.*, 2005; Park *et al.*, 2006; Prass *et al.*, 2006). Here, we show that correlation and Fourier analysis of membrane fluctuations of stationary human fibroblasts reveal distinct mechanical pulsations which have time constants that vary spatially and temporally. We compare our analysis with measurements on rat CMs that are known to display highly correlated motions. Finally, we show that it is possible to distinguish between interphase cells, cells treated with anti-cytoskeletal drugs, and early apoptotic cells based solely on the correlation time constants of the membrane fluctuations and pulsations. Correlation and Fourier analysis provides a way to uniquely identify physiological states based on non-random mem-

brane fluctuation which also appears to be cell type dependent.

MATERIALS AND METHODS

Primary neonatal rat CMs

CMs were prepared as previously described (Mathur *et al.*, 2000). Hearts were dissected from 3 to 4 day old Sprague–Dawley rat pups and washed in oxygenated ADS buffer (116 mM NaCl, 5.4 mM KCl, 0.4 mM MgSO₄, 5.5 mM D-Glucose, 0.8 mM NaH₂PO₄, 20 mM HEPES, pH 7.4), followed by cutting into small ~ 1 mm² sections. The tissue was then digested in 0.03% collagenase (Worthington Biochemicals)/0.06% pancreatin (Sigma) dissolved in ADS, for 15 min and the supernatant discarded. The digestion was then repeated six more times while collecting the supernatant that contained the released cells. Dissociated cells were plated on 100 mm tissue culture dishes (Falcon) in plating media (68% DMEM (Invitrogen), 17% Medium 199 (Invitrogen), 10% Horse Serum (Invitrogen), 5% FBS (Sigma), 100 IU/mL penicillin and 100 μ g/mL streptomycin (Sigma)) for 1 h at 37°C/5% CO₂. The non-adherent CMs were then collected and plated in 60 mm culture dishes (Falcon) at a density of $\sim 2 \times 10^5$ cells/cm². After 24 h cells were switched to maintenance media (80% DMEM, 19% Medium 199, 1% FBS, antibiotics (as above) and 50 μ M 5-bromo-2-deoxyuridine (Sigma)). Cells were cultured 4 days and used between days 5 and 7.

Human neonatal foreskin fibroblasts and drug treatments

Human foreskin fibroblasts (HFFs) (Karocell) were cultured in DMEM with GlutaMAX, supplemented with 10% heat inactivated FBS, 1% non-essential amino acids, 0.1 mM β mercaptoethanol (all from Invitrogen), 100 IU/mL penicillin and 100 μ g/mL streptomycin (BioWhittaker Inc.). The cells were seeded on 60 mm culture dishes (Corning) and were maintained at 37°C and 5% CO₂. Apoptosis was induced by exposing the cells to 4 μ M Staurosporine (STS) (Sigma) for 2 h prior to measurements (Mannherz *et al.*, 2006). Cells were sometimes treated with Cytochalasin D (CytD) or Nocodazole (Sigma) at 10 μ M for 1 h prior to measurements.

AFM and motion analysis

Cells were mounted on a temperature controlled stage at 37°C of a combined AFM–fluorescence microscope (Olympus IX70 inverted optical microscope with a JPK NanoWizard AFM (JPK Instruments)). Untreated MSC1-AUHW AFM cantilevers (Veeco), stored in a desiccated chamber, were used for all motion analysis and had experimentally determined (Levy and Maaloum, 2002) spring constants of 0.02 ± 0.01 N/m. Cantilevers used during drug treatments were only used once to avoid cross-contamination. The AFM cantilever was brought into stationary contact with an optically chosen cell at an

applied force of 0.5 nN. Similar to previous work (Pelling *et al.*, 2004; Pelling *et al.*, 2005), the vertical error signal ($x(t)$) was collected from the photodiode with custom LabView software but at a low sampling rate of 100 Hz and low pass filtered at 58 Hz.

The motion data were examined with Fourier and autocorrelation analysis carried out using custom MatLab scripts. 2D autocorrelation plots were generated with Origin software (OriginLab). The autocorrelation function (ACF or $C(\tau)$) is a powerful tool because it is capable of recovering non-random components buried underneath data which appear to be completely random. The ACF is defined as:

$$C(\tau) = \lim_{T \rightarrow \infty} \frac{1}{2T} \int_{-T}^T x(t)x(t + \tau)dt$$

where $x(t)$ is a stochastic stationary ergodic process, τ is the so-called Lag time, $C(\tau)$ is an even function of τ and $C(0) \geq |C(\tau)|$. This means that the ACF will have its greatest value at zero lag, the mean-square variance of $x(t)$, and in the absence of non-random periodic processes the ACF will be asymptotic around $\tau = 0$. For large τ , the ACF will approach zero as values separated over a large period of time should not be correlated. However, if there are non-random processes buried inside $x(t)$ the ACF will decay much more slowly than a truly random process and possibly display periodic characteristics. A powerful property of the ACF is that the FT of the ACF provides us with the auto power spectrum $S(f)$ (Weiner–Kintchine theorem). Therefore, if measurements are only made during interphase using the error signal and assuming the biomechanical mechanisms causing the membrane fluctuations remain constant during this time we can use the Weiner–Kintchine theorem:

$$S(f) = 4 \int_0^{\infty} C(\tau) \cos(2\pi f\tau) d\tau$$

$$C(\tau) = \int_0^{\infty} S(f) \cos(2\pi f\tau) df$$

$S(f)$ and $C(\tau)$ are cosine FT pairs and $S(f)$ is effectively a ‘filtered’ spectrum as calculation of the ACF has removed random components. This is clearly advantageous over applying an FT directly on the raw data which include both random and non-random components of the data.

Fluorescence staining, apoptosis assay and microscopy

Cells were rinsed with PBS, fixed with a 3.5% paraformaldehyde, 2% sucrose solution and then permeabilized with 0.5% Triton-X100 at 37°C. Samples were then sequentially incubated with Phalloidin-TRITC (Sigma), monoclonal anti- α -tubulin (Sigma) and FITC conjugated polyclonal rabbit anti-mouse immunoglobins (Dako) and incubated in wash buffer (5% Normal Calf Serum, 0.05% Azide in PBS) for 30 min after each step on ice. Finally, the cells were rinsed in PBS three times and mounted in glycerol. An Apoptosis Detection Kit (Biovision) was used to carry out an Annexin V-FITC/propidium iodide (PI) assay according to the manufacturer protocol (Ohshima, 2006). Cells were stained, fixed as above and immediately imaged. Fluor-

escence microscopy was carried out with the Olympus inverted IX70 fluorescence microscope of the JPK AFM using a 40 \times objective, appropriate filters and a Hamamatsu Deep Cooled CCD Camera (ORCA-AG, Hamamatsu). Images were analysed with Wasabi software and contrast optimized to maximize the fluorophore signal.

RESULTS

Autocorrelation and Fourier analysis of membrane fluctuations of CMs and fibroblasts

In order to measure local membrane fluctuations cells were placed in the AFM and a cell was chosen optically (Wu *et al.*, 1998). The AFM tip was then brought into contact with the cell and the vertical deflections of the cantilever were recorded. In a control case, we measured the mechanical fluctuations of primary neonatal rat CMs (Figure 1A) (Haupt *et al.*, 2006). Contractions were observed with average amplitudes of ~ 3 nN and at frequencies of ~ 4.2 Hz, as determined from a direct Fourier transform (FT) and consistent with previous work (Shroff *et al.*, 1995; Domke *et al.*, 1999; Haupt *et al.*, 2006).

For periodic contractions of CMs we can calculate a normalized ACF ($C_n(\tau) = C(\tau)/C(0)$) in order to compare with data measured on different cells (Figure 1B). In the case of CM motion ($n = 5$), the ACF decays to zero but maintains highly periodic dynamics. The ACF becomes anti-correlated every ~ 0.12 s, or the time between the maxima and minima of the contractions. FT of the ACF provides the principle beating frequency (and the characteristic correlation time constant $t_c = 1/f = \sim 0.24$ s) (Figure 1C).

Membrane fluctuations of stationary interphase HFF cells ($n = 21$) were observed to be smaller in amplitude and displayed occasional mechanical pulsations (20–100 pN amplitudes) (Figure 1D) in which the membrane expanded upwards and contracted back to a baseline position (Szabo *et al.*, 2002). Between pulsations, the motion was non-periodic and the baseline motion appeared random with fluctuations of ~ 10 –20 pN. The background fluctuations of the AFM system were determined by measuring the substrate motion near the cell of interest. The measured bandwidth limited background fluctuations (~ 1 –5 pN rms, after 58 Hz low pass filtering) are below the motions observed at the cell membrane and never displayed any periodicity (Figure 1E). Importantly, the culture dish ($n = 5$) had an average ACF which was asymptotic around $\tau = 0$, demonstrating truly random data. This is in comparison to the average ACF of interphase cells which displayed both negative and positive correlations over long time scales (>10 s). These are quantified in the FT (Figure 1F) which can be used to calculate the t_c 's which describe the motion (Table 1). The FT of the raw data (no ACF calculation) is also shown and although four broad components are visible, the resolution is clearly enhanced after filtering out random noise with the ACF. Three t_c 's at 6.33 ± 1.08 , 3.92 ± 0.43 and 2.95 ± 0.19 s are directly related to the dynamics of the mechanical pulsations, however it is clear that long time scale correlations (16.39 ± 2.69 s) are occurring and may be driven by multiple mechanisms (Szabo *et al.*, 2002).

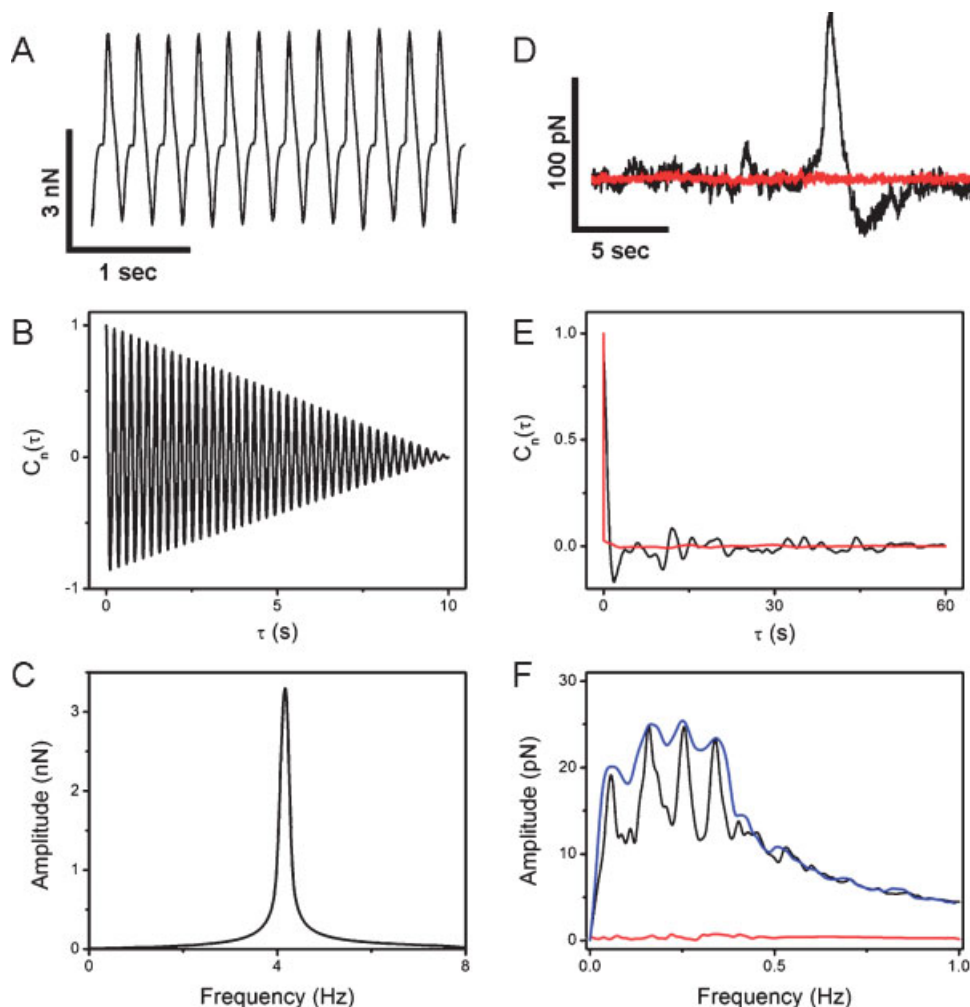


Figure 1. Motion, autocorrelation and Fourier analysis of CM and HFF cells reveal characteristic time constants and frequencies. CMs display typical vertical contractions (A) and corresponding oscillations in the normalized ACF (B). FT of the ACF reveals the principle beating frequency at ~ 4.2 Hz (C). HFF cells (black) display occasional mechanical pulsations in comparison to the control Petri dish (red) (D). The ACF (E) of the Petri dish (red) reveals the motion is completely random, whereas the cell (black) has several non-random components related to the mechanical pulsations. An FT of the respective ACFs (F) reveal characteristic frequencies in the motion measured on the HFF cell (black) and none for the Petri dish (red). The blue line is the direct FT of the raw data without ACF calculation which clearly shows a significant enhancement in resolution. In all data, motion was measured on several individual cells, the ACF calculated for each and the average ACF presented. FT of the average ACF then provides the average spectrum under each set of conditions.

Table 1. Frequencies (above) and calculated time constants (below)

	Component 1	Component 2	Component 3	Component 4	Component 5
Interphase	nc	0.06 ± 0.01 Hz 16.39 ± 2.69 s	0.15 ± 0.03 Hz 6.33 ± 1.08 s	0.26 ± 0.03 Hz 3.92 ± 0.43 s	0.34 ± 0.02 Hz 2.95 ± 0.19 s
CytD	0.03 ± 0.01 Hz 32.26 ± 5.20 s	0.09 ± 0.03 Hz 10.64 ± 2.83 s	0.18 ± 0.02 Hz 5.43 ± 0.50 s	0.30 ± 0.01 Hz 3.3 ± 0.10 s	nc
Nocodazole	0.03 ± 0.01 Hz 30.30 ± 7.35 s	0.11 ± 0.02 Hz 9.09 ± 1.90 s	0.19 ± 0.01 Hz 5.21 ± 0.33 s	0.27 ± 0.01 Hz 3.37 ± 0.19 s	0.36 ± 0.01 Hz 2.82 ± 0.09 s
STS	0.03 ± 0.01 Hz 35.71 ± 11.48 s	0.07 ± 0.01 Hz 14.49 ± 2.31 s	0.15 ± 0.01 Hz 6.76 ± 0.41 s	nc	nc

Values are grouped according to similar non-random components (nc = no component).

Analysis of membrane fluctuations after exposure to anti-cytoskeletal drugs and during early apoptosis

To understand the mechanism causing the characteristic t_c and to determine if it is possible to distinguish specific changes in physiological state, we performed three further experiments. The actin or microtubule (MT) filament systems were depolymerized with the well-known anti-cytoskeletal drugs CytD and Nocodazole, respectively. To determine if membrane fluctuations could be linked to physiological state we induced early apoptosis with the well-known protein-kinase inhibitor STS (Mannherz *et al.*, 2006). Fluorescence microscopy was performed in order to determine the underlying architectural changes associated with exposure to each drug (Figure 2). In interphase cells, F-actin forms a network of long filaments spanning the length of the cell whereas MTs are found as a dense meshwork of filaments throughout the cytoplasm (Figure 2A, B). After treatment with CytD for 1 h, F-actin completely depolymerized, while the MT filaments were intact but condensed with the shrinking cell (Figure 2C, D). On the other hand, Nocodazole depolymerized MTs while leaving F-actin intact (Figure 2E, F). STS induced distinct structural changes after exposure for 2 h (Mannherz *et al.*, 2006). F-actin is found completely depolymerized and in complex stellate structures, while the MT network remained intact surrounding the nucleus (Pelling *et al.* Unpublished results). STS was confirmed to induce early apoptosis after 2 h, and not necrosis, with a standard Annexin V-FITC/PI assay. Cells were Annexin V-FITC positive and PI negative (Figure 3) indicating significant amounts of phosphatidyl serine on the outer leaflet of the intact membrane (Ohshima, 2006).

After treatment with the respective drugs, membrane motion was recorded and the average ACF and power spectra were calculated. Notably, CytD and Nocodazole treated cells retained the ability to display distinct pulsations with amplitudes varying between 20 and 80 pN. STS cells displayed only small movements (<20 pN) which were very

close to the level of the noise (Figure 4A). These differences in membrane fluctuations were captured in the average ACFs for CytD ($n=21$), Nocodazole ($n=21$) and STS ($n=12$) treated cells which are clearly distinct from each other (Figure 4B) and in comparison to the interphase cells. The CytD and Nocodazole ACFs both became anti-correlated, followed by a recovery and becoming uncorrelated. The CytD ACF displayed periodic characteristics during the recovery whereas the Nocodazole ACF is more complex. The STS ACF is clearly distinguishable from the CytD and Nocodazole ACFs. It becomes uncorrelated without becoming anti-correlated or distinctly periodic, which only arises from the mechanical pulsations. Importantly, the decay in the ACF is much slower than purely random motion (Figure 1E).

FT of the ACFs revealed characteristic power spectra for each drug (Figure 4C). Time constants derived from these spectra are summarized in Table 1. Normalized spectra, shifted for comparison, can be used to determine distinct spectral features (Figure 4C, inset) which are worth discussion here. The CytD, Nocodazole and STS treated cells all displayed a small low-frequency peak at ~ 0.03 Hz (~ 33 s) not found in the interphase cell. The peak is more pronounced in Nocodazole and STS treated cells, while it appeared as a broad shoulder in CytD treated cells. CytD- and Nocodazole treated cells also had a broad second peak (0.09 and 0.11 Hz, respectively) which fell in between peak 1 (~ 0.06 Hz) and peak 2 (~ 0.15 Hz) of the interphase cell. Interphase and Nocodazole treated cells displayed two peaks at ~ 0.26 , ~ 0.34 Hz and ~ 0.27 , ~ 0.36 Hz respectively. These peaks are not found in CytD and STS treated cells which are without intact F-actin. CytD treated cells had a peak at ~ 0.30 Hz which is roughly between the two peaks observed in interphase and Nocodazole treated cells. Finally, STS treated cells only display low frequency peaks below ~ 0.15 Hz which corresponds to time constants longer than ~ 7 s. Therefore, time constants <7 s are likely related to the dynamics of the distinct mechanical pulsations.

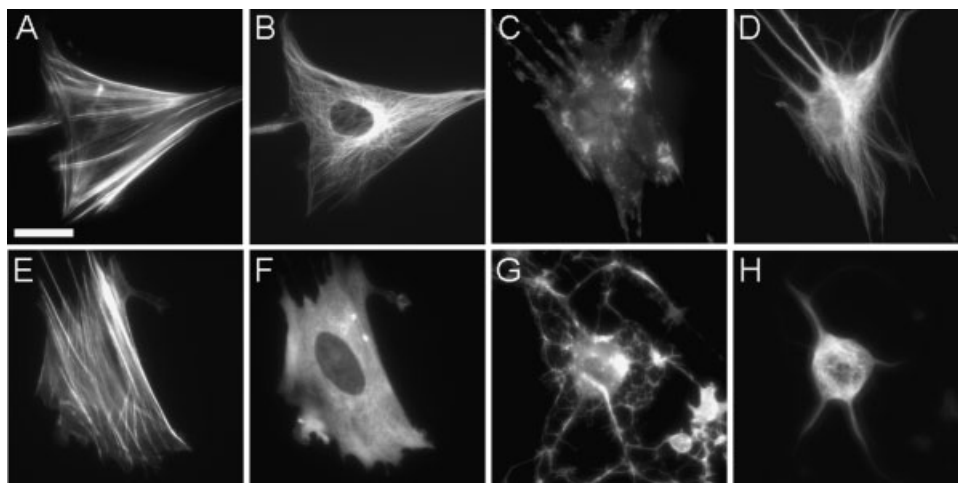


Figure 2. Fluorescence microscopy of the actin and microtubule (MT) cytoskeletons in interphase (A, B), CytD treated (C, D), Nocodazole treated (E, F) and STS treated (G, H) cells, respectively. CytD clearly depolymerizes F-actin while leaving MTs intact, whereas Nocodazole completely depolymerizes MTs, leaving F-actin intact. Apoptotic STS treated cells possess depolymerized F-actin and highly condensed, but intact MTs. Scale bar = 20 μ m.

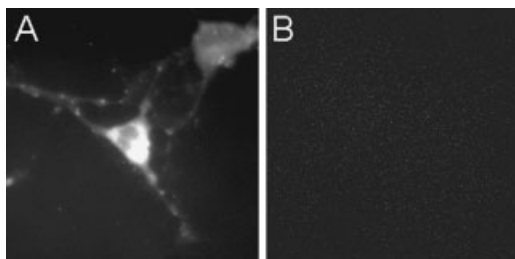


Figure 3. STS induces early apoptosis as confirmed with an Annexin V-FITC/PI assay. The cell is positive for external PS on the cell membrane (A). However, the plasma membrane is still intact (B), blocking PI from entering the cell nucleus and becoming fluorescent which produces a black image. Images are $80 \mu\text{m}^2$.

Two-dimensional (2D) autocorrelation plots for healthy fibroblasts

In a method similar to force-volume imaging (Rotsch and Radmacher, 2000), we measured membrane fluctuations at positions in a 5×5 grid over a $10 \mu\text{m}^2$ area above the

nucleus of interphase cells (Figure 4D). At each point, fluctuations were recorded for 30 s, followed by calculation of ACF's and power spectra. Therefore, for a given time constant, the peak amplitude can be spatially mapped at each position over the $10 \mu\text{m}^2$ area. This produces four spatial autocorrelation plots (SAPs) for the interphase cell allowing us to examine their spatial relationship (Figure 5). Similar to force-volume imaging, SAPs are not 'snap shots' of correlation time constants as it takes ~ 13 min to acquire the data. However, for stationary interphase HFF cells, no significant change in morphology was observed during this period. Admittedly, quantitative phase imaging (Popescu *et al.*, 2006) allow for a faster, higher resolution and more direct determination of spatial correlations; but the AFM approach presented here provides force information and spatial insights without the need for an advanced optical setup.

Generally, for a given time constant, an area of large amplitude corresponded to areas of large amplitude of the other three time constants. For example, in Figure 5A the time constant ($\tau = 2.95$ s) has a peak at the (x,y) -coordinates,

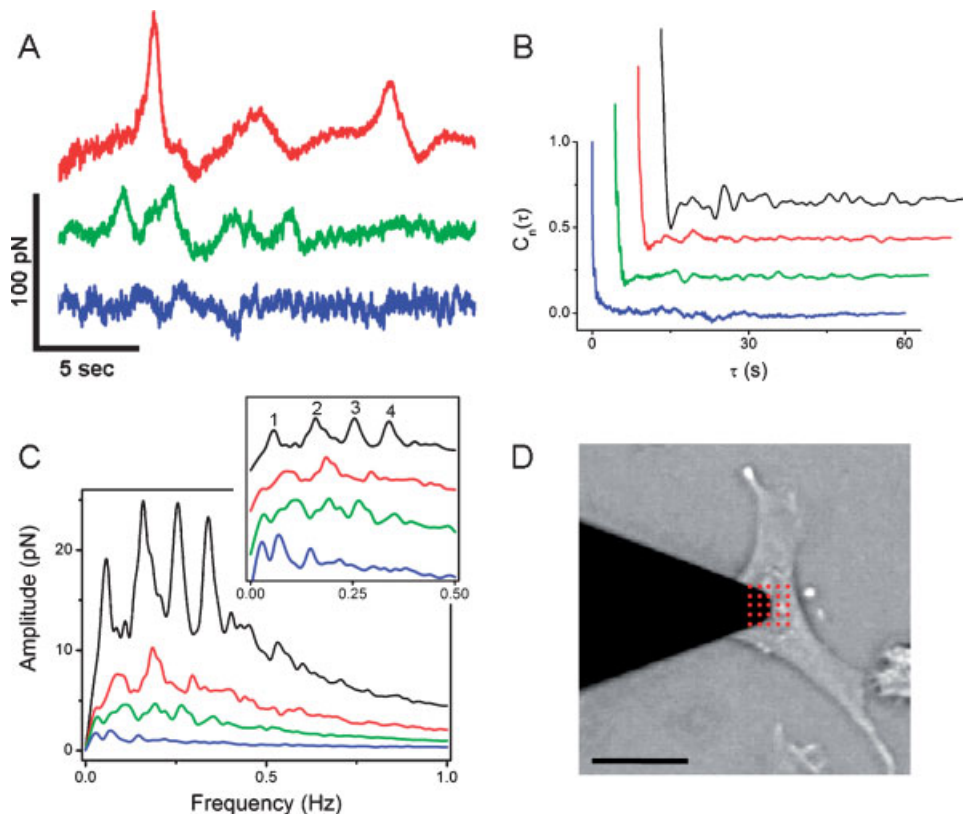


Figure 4. Motion, autocorrelation and Fourier analysis of cells treated with CytD (red), Nocodazole (green) and STS (blue) (colours apply to A–C). Membrane motion (A) of the cells reveal mechanical pulsations (20–80 pN) occurring after cytoskeleton depolymerization. However, in STS cells large pulsations are no longer observed and only small amplitude (< 20 pN) fluctuations occur. The ACFs after drug treatments are shown together in a waterfall plot (B). Each ACF is clearly distinguishable from the interphase cell (black, data replotted from Figure 1E and applies to C). FT of the ACFs (C) reveal characteristic frequencies occurring after drug treatment, revealing that each physiological state can be distinguished from each other and from interphase cells. Inset: normalized spectra shifted for comparison allow specific frequency components to be identified (the four principle peaks are labelled for the interphase cell). Spatial autocorrelation plots (SAPs) were generated by moving the tip to positions in a 5×5 grid (red dots mark the positions) over the nucleus of a living cell and measuring membrane fluctuations (D). In the phase-contrast image (scale bar = $20 \mu\text{m}$) the nucleus is visible under the AFM tip. The tip is sequentially moved to each point using force-volume positioning control.

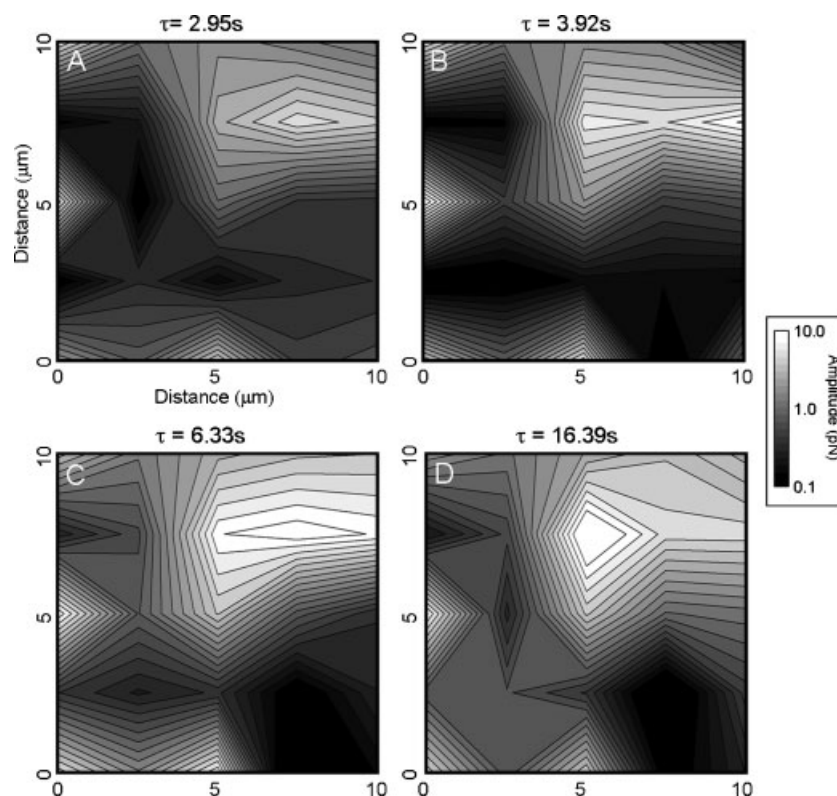


Figure 5. SAPs for one representative interphase cell; however, similar trends were observed in all cells measured ($n=5$). The amplitude of each characteristic time constant is measured and plotted over a $10\ \mu\text{m}^2$ area. Clearly, the membrane pulsations and characteristic time constants vary spatially and are not always directly related. The SAP is not a 'snap shot' of correlated membrane motion but does provide some insight into the spatial variability of the measurement.

($7.5\ \mu\text{m}$, $7.5\ \mu\text{m}$). Large amplitudes in that region are also observed for the other time constants, $\tau=3.92$, 6.33 and 16.39 s (Figure 5B–D). However, the location of the maxima in each region varies between SAPs. The maximum is shifted to the left ($5.0\ \mu\text{m}$, $7.5\ \mu\text{m}$) in Figure 5D when compared to Figure 5A, C, and there are two peaks in Figure 5B at ($5.0\ \mu\text{m}$, $7.5\ \mu\text{m}$) and ($10.0\ \mu\text{m}$, $7.5\ \mu\text{m}$). Furthermore, in Figure 5B three large minima were observed at ($2.5\ \mu\text{m}$, $7.5\ \mu\text{m}$), ($2.5\ \mu\text{m}$, $2.5\ \mu\text{m}$) and ($7.5\ \mu\text{m}$, $2.5\ \mu\text{m}$). In contrast, only one large minimum is observed at ($7.5\ \mu\text{m}$, $2.5\ \mu\text{m}$) in Figure 5C, D. Finally, in Figure 5A three minima occur but in different locations ($2.5\ \mu\text{m}$, $5.0\ \mu\text{m}$), ($0.0\ \mu\text{m}$, $2.5\ \mu\text{m}$) and ($5.0\ \mu\text{m}$, $2.5\ \mu\text{m}$). Clearly, the time constants on the cell membrane vary both spatially and temporally and are not always co-dependent.

DISCUSSION AND CONCLUSIONS

We have shown in this study that it is possible to measure nanomechanical membrane fluctuations in eukaryotic cells, primary CMs and fibroblast cell lines, in a manner similar to previous work (Shroff *et al.*, 1995; Domke *et al.*, 1999; Rotsch *et al.*, 1999; Szabo *et al.*, 2002; Pelling *et al.*, 2004; Pelling *et al.*, 2005; Haupt *et al.*, 2006). The membrane fluctuations contained transient mechanical pulsations occurring one to three times *per* minute, separated by

periods of quiescence with baseline amplitudes of <20 pN. Employing autocorrelation and Fourier analysis we have shown that we can extract characteristic time constants which describe the membrane fluctuations which clearly depend on physiological state. These components can either be related to the dynamics of the observed mechanical pulsations or to longer timescale motions, but it is difficult to accurately assign each peak in the observed spectra. The mechanical pulsations display multiple component frequencies varying between 0.1 and 0.5 Hz. Notably, two peaks in the interphase FT (~ 0.26 and ~ 0.34 Hz) are also present in the Nocodazole FT (~ 0.27 and ~ 0.36 Hz) but not in the CytD or STS treated cells. Since intact F-actin was not present in CytD or STS treated cells, we can tentatively assign these two peaks to actin driven dynamics: specifically, actin–myosin contractions and/or polymerization dynamics which tend to fall in the observed frequency range (Shroff *et al.*, 1995; Yasuda *et al.*, 1996; Domke *et al.*, 1999; Szabo *et al.*, 2002). Transient low frequency membrane oscillations or mechanical pulsations have been observed in non-muscle cells previously (Bornens *et al.*, 1989; Ehrenguber *et al.*, 1996; Pletjushkina *et al.*, 2001; Szabo *et al.*, 2002) and appear to be driven by Rho-kinase activity (Pletjushkina *et al.*, 2001). This is in agreement with this work, as STS can inhibit on Rho-kinase (Amano *et al.*, 1997) resulting in the loss of mechanical pulsations, although low frequency components

can clearly be extracted with the ACF from random fluctuations.

The long timescale motions are difficult to assign to specific cellular activities. In spreading or migrating cells, slow MT dependent oscillations have been observed in which the cell moves back and forth with periods of ~ 50 s (Bornens *et al.*, 1989; Ehrenguber *et al.*, 1996; Pletjushkina *et al.*, 2001). This corresponds to a frequency of ~ 0.02 Hz which is similar to the observed component at ~ 0.03 Hz in this study. This peak was only observed in cells where one cytoskeletal filament system had been depolymerized. In Nocodazole treated cells this peak is enhanced compared to CytD treated cells (Pletjushkina *et al.*, 2001). However, apoptotic cells also display this peak which may be related to the loss of focal adhesions and a slow rocking of the rounded cell body. Regardless, we speculate that long correlation times are related to the natural dynamics of the plasma membrane or cell body. When the cytoskeleton is completely intact, the membrane is highly linked to the cytoskeleton and cortical tension is high. Pronounced dynamics occur over short time scales appear to be related to cytoskeletal activity, consistent with previous work (Szabo *et al.*, 2002; Gov and Safran, 2005; Popescu *et al.*, 2005; Gov and Gopinathan, 2006; Popescu *et al.*, 2006; Silva *et al.*, 2006). These dynamics are dependent on the viability of the cell, as early apoptotic cells display no mechanical pulsations even though they have an intact tubulin cytoskeleton and in contrast to Nocodazole treated cells.

We also observed that the amplitude of the observed frequency components vary spatially over the cell membrane when examined with SAPs. Elegant work on erythrocytes using quantitative phase imaging has also revealed highly dynamic and spatially varying fluctuations of cell membranes (Popescu *et al.*, 2005; Popescu *et al.*, 2006). These results show the importance of actin dynamics in governing cell membrane fluctuations. However, the results presented here on CytD or STS treated cells clearly show that membrane pulsations and fluctuations can occur with characteristic frequencies; this highlights both the role of MTs and the likely influence of other, unknown pathways that may involve intermediate filaments or links between individual cytoskeletal filaments and the membrane.

Finally, our work on HFF cells appears to demonstrate that the membrane fluctuations may be cell type dependent. Preliminary measurements on interphase 3T3 fibroblasts revealed a set of characteristic t_c 's different from the interphase HFF cells (data not shown). However, a variety of stable or spreading cell types either display no deterministic fluctuations or membrane oscillations (CM's in this work) with very different dynamics to those observed here (Shroff *et al.*, 1995; Domke *et al.*, 1999; Rotsch *et al.*, 1999; Pletjushkina *et al.*, 2001; Szabo *et al.*, 2002; Pelling *et al.*, 2004; Pelling *et al.*, 2005; Popescu *et al.*, 2005; Popescu *et al.*, 2006; Silva *et al.*, 2006). Our work has shown that these measurements can also be linked to the physiological state of a cell, as apoptotic cells have clearly different spectra. Several methods have been used to examine membrane motion in many cells types and it is now clear that the cytoskeleton is an important factor in determining mechanical dynamics. Although these methods have become highly attractive because of the obvious utility in cellular diagnostics, the deeper biological mechanisms behind these phenomena have remained elusive. It is still unknown how a non-muscle cell benefits from driving low frequency oscillations of its cell membrane. As well, the motion is not a purely physical phenomenon as the fluctuations appear to be metabolically driven and related to internal Rho protein signalling pathways (Pletjushkina *et al.*, 2001). Therefore, uncovering the basis of this mechanical activity is crucial for understanding how it may be exploited, which will have important implications for future nanomedicines and diagnostics.

Acknowledgments

A. E. P. and M. A. H. would like to acknowledge the IRC in Nanotechnology (Cambridge, UCL and Bristol, EPSRC, UK) for financial support through a generous Exploratory Research Grant. M. A. H. is supported by the Wellcome Trust. C. C. thanks the BBSRC for support. A. H. thanks the EPSRC and the UK Stem Cell Bank, NIBSC. A. E. P., B. M. N. and M. A. H. are especially grateful to Dr. Buket Demirci and Prof. Anthony Mathur (Bart's and The London, Queen Mary's School of Medicine and Dentistry) for helping us to establish the cardiomyocyte isolation and culture protocol.

REFERENCES

- Amano M, Chihara K, Kimura K, Fukata Y, Nakamura N, Matsuura Y, Kaibuchi K. 1997. Formation of actin stress fibers and focal adhesions enhanced by rho-kinase. *Science* **275**: 1308–1311.
- Bechhoefer J, Wilson S. 2002. Faster, cheaper, safer optical tweezers for the undergraduate laboratory. *Am. J. Phys.* **70**: 393–400.
- Binnig G, Quate CF, Gerber C. 1986. Atomic force microscope. *Phys. Rev. Lett.* **56**: 930–933.
- Bornens M, Paintrand M, Celati C. 1989. The cortical microfilament system of lymphoblasts displays a periodic oscillatory activity in the absence of microtubules: implications for cell polarity. *J. Cell. Biol.* **109**: 1071–1083.
- Brown FL. 2003. Regulation of protein mobility via thermal membrane undulations. *Biophys. J.* **84**: 842–853.
- Domke J, Parak WJ, George M, Gaub HE, Radmacher M. 1999. Mapping the mechanical pulse of single cardiomyocytes with the atomic force microscope. *Eur. Biophys. J.* **28**: 179–186.
- Ehrenguber MU, Deranleau DA, Coates TD. 1996. Shape oscillations of human neutrophil leukocytes: characterization and relationship to cell motility. *J. Exp. Biol.* **199**: 741–747.
- Gov N. 2004. Membrane undulations driven by force fluctuations of active proteins. *Phys. Rev. Lett.* **93**: 268104.
- Gov NS, Gopinathan A. 2006. Dynamics of membranes driven by actin polymerization. *Biophys. J.* **90**: 454–469.
- Gov NS, Safran SA. 2005. Red blood cell membrane fluctuations and shape controlled by atp-induced cytoskeletal defects. *Biophys. J.* **88**: 1859–1874.
- Haupt BJ, Pelling AE, Horton MA. 2006. Integrated confocal and scanning probe microscopy for biomedical research. *Scientific World J.* **6**: 1609–1618.

- Levy R, Maaloum M. 2002. Measuring the spring constant of atomic force microscope cantilevers: thermal fluctuations and other methods. *Nanotechnology* **13**: 33–37.
- Lin LC, Gov N, Brown FL. 2006. Nonequilibrium membrane fluctuations driven by active proteins. *J. Chem. Phys.* **124**: 74903.
- Mannherz HG, Gonsior SM, Wu X, Polzar B, Pope BJ, Wartosch L, Weeds AG. 2006. Dual effects of staurosporine on a431 and nrk cells: microfilament disassembly and uncoordinated lamellipodial activity followed by cell death. *Eur. J. Cell. Biol.* **85**: 785–802.
- Mathur A, Hong Y, Kemp BK, Barrientos AA, Erusalimsky JD. 2000. Evaluation of fluorescent dyes for the detection of mitochondrial membrane potential changes in cultured cardiomyocytes. *Cardiovasc. Res.* **46**: 126–138.
- Ohshima S. 2006. Apoptosis and necrosis in senescent human fibroblasts. *Ann. NY Acad. Sci.* **1067**: 228–234.
- Park YK, Popescu G, Badizadegan K, Dasari RR, Feld MS. 2006. Diffraction phase and fluorescence microscopy. *Opt. Exp.* **14**: 8263–8268.
- Pelling AE, Sehati S, Gralla EB, Valentine JS, Gimzewski JK. 2004. Local nanomechanical motion of the cell wall of *Saccharomyces cerevisiae*. *Science* **305**: 1147–1150.
- Pelling AE, Sehati S, Gralla EB, Valentine JS, Gimzewski JK. 2005. Time dependence of the frequency and amplitude of the local nanomechanical motion of yeast. *Nanomedicine* **1**: 178–183.
- Pelling AE, Dawson DW, Carreon DM, Christiansen JJ, Shen RR, Teitell MA, Gimzewski JK. 2007. Distinct contributions of microtubule subtypes to cell membrane shape and stability. *Nanomedicine* **3**: 43–52.
- Pletjushkina OJ, Rajfur Z, Pomorski P, Oliver TN, Vasiliev JM, Jacobson KA. 2001. Induction of cortical oscillations in spreading cells by depolymerization of microtubules. *Cell. Motil. Cytoskeleton* **48**: 235–244.
- Popescu G, Ikeda T, Best CA, Badizadegan K, Dasari RR, Feld MS. 2005. Erythrocyte structure and dynamics quantified by hiltbert phase microscopy. *J. Biomed. Opt.* **10**: 060503.
- Popescu G, Badizadegan K, Dasari RR, Feld MS. 2006. Observation of dynamic subdomains in red blood cells. *J. Biomed. Opt.* **11**: 040503.
- Prass M, Jacobson K, Mogilner A, Radmacher M. 2006. Direct measurement of the lamellipodial protrusive force in a migrating cell. *J. Cell. Biol.* **174**: 767–772.
- Rotsch C, Radmacher M. 2000. Drug-induced changes of cytoskeletal structure and mechanics in fibroblasts: an atomic force microscopy study. *Biophys. J.* **78**: 520–535.
- Rotsch C, Jacobson K, Radmacher M. 1999. Dimensional and mechanical dynamics of active and stable edges in motile fibroblasts investigated by using atomic force microscopy. *Proc. Natl. Acad. Sci. USA* **96**: 921–926.
- Shroff SG, Saner DR, Lal R. 1995. Dynamic micromechanical properties of cultured rat atrial myocytes measured by atomic force microscopy. *Am. J. Physiol.* **269**: C286–292.
- Silva HS, Martins ML, Vilela MJ, Jaeger R, Kachar B. 2006. 1/f ruffle oscillations in plasma membranes of amphibian epithelial cells under normal and inverted gravitational orientations. *Phys. Rev. E* **74**: 041903-1–041903-8.
- Smith SB, Cui Y, Bustamante C. 2003. Optical-trap force transducer that operates by direct measurement of light momentum. *Methods Enzymol.* **361**: 134–162.
- Strick TR, Allemand JF, Bensimon D, Croquette V. 2000. Stress-induced structural transitions in DNA and proteins. *Annu. Rev. Biophys. Biomol. Struct.* **29**: 523–543.
- Szabo B, Selmeczi D, Kornyei Z, Madarasz E, Rozlosnik N. 2002. Atomic force microscopy of height fluctuations of fibroblast cells. *Phys. Rev. E Stat. Nonlin. Soft. Matter. Phys.* **65**: 041910.
- Tishler RB, Carlson FD. 1987. Quasi-elastic light scattering studies of membrane motion in single red blood cells. *Biophys. J.* **51**: 993–997.
- Tishler RB, Carlson FD. 1993. A study of the dynamic properties of the human red blood cell membrane using quasi-elastic light-scattering spectroscopy. *Biophys. J.* **65**: 2586–2600.
- Tuvia S, Moses A, Gulayev N, Levin S, Korenstein R. 1999. Beta-adrenergic agonists regulate cell membrane fluctuations of human erythrocytes. *J. Physiol.* **516**: 781–792.
- Wu HW, Kuhn T, Moy VT. 1998. Mechanical properties of 1929 cells measured by atomic force microscopy: effects of anticytoskeletal drugs and membrane crosslinking. *Scanning* **20**: 389–397.
- Yasuda K, Shindo Y, Ishiwata S. 1996. Synchronous behavior of spontaneous oscillations of sarcomeres in skeletal myofibrils under isotonic conditions. *Biophys. J.* **70**: 1823–1829.